Electronic Supplementary Material (ESI) for RSC Advances

Support Information

Graphene/aramid nanofiber nanocomposite paper with high mechanical and electrical performances

Jinchen Fan [a], Zixing Shi [*a], and Jie Yin [a]

[a] School of Chemistry and Chemical Engineering & State Key Laboratory for Metal Matrix Composite Materials, Shanghai Jiao Tong University, 200240, Shanghai, People's Republic of China

---

[*] Corresponding author. E-mail address: zxshi@sjtu.edu.cn (Z. Shi).

Tel: +86 21 54743268, Fax: +86 21 54747445

1 Preparation of graphite oxide

Graphite oxide was obtained by a modified Hummers method[1, 2]. In brief, Graphite powder (3 g, 325 mesh), $K_2S_2O_8$ (2.5 g), and P_2O_5 (2.5 g) were added into the concentrated H_2SO_4 (20 mL). After reaction of 4.5 h at 80 °C, the mixture solution was cooled to room temperature and diluted with 0.5 L of de-ionized (DI) water and left overnight. Then, the mixture was filtered and washed with de-ionized (DI) water to remove the residual acid. The product was dried under ambient condition overnight. This pre-oxidized graphite was then subjected to oxidation by Hummers' method described as follows. Pretreated graphite powder was put into cold (0 °C) concentrated H_2SO_4 (120 mL). Then, $KMnO_4$ (15 g) was added gradually under stirring and the temperature of the mixture was kept to be below 20 °C by cooling. Successively, the mixture was stirred at 35 °C for 2 h, and then diluted with DI water (250 mL) under ice bath. Successively, the mixture solution was stirred for 2 h. After the reaction, the mixture solution was poured into 1 L deionized water, 20 mL of 30% H_2O_2 was added to the mixture solution. The mixture solution was centrifuged and washed with 1:10 HCl aqueous solution six times and deionized water four times. Then, the obtained graphite oxide was lyophilized in a freeze–dry system for 1 week to remove water completely.

2 Graphene oxide/dimethylsulfoxide (GO/DMSO) dispersion

The GO/DMSO dispersion was prepared *via* solvent-exchange[3, 4]. Briefly, 0.5 g of graphite oxide was exfoliated and dispersed in 100 mL water for 4 h by sonication. Then, 100 mL DMSO was added to the graphene oxide aqueous dispersion and further sonicated for 1 h. After that, the water was totally removed by vacuum distillation until a portion of DMSO started to distill out. A certain volume of the GO/DMSO dispersion was dried at 80 ^{o}C and weighted to determine the final concentration of GO of the GO/DMSO dispersion.

3 Preparation of ANFs/DMSO dispersion

The aramid nanofibers (ANFs) solution was prepared by the method presented by Kotov's group[5]. 1.0 g of Kevlar 49 fibers and 1.5 g KOH were added into 500 mL of DMSO. After magnetic stirring for one week at room temperature, a dark red ANF/DMSO dispersion (2 mg/ml) was finally obtained.

4 Fabrication of RGO/ANFs nanocomposite paper

4.1 GO/ANFs nanocomposite paper

Desired amount of GO/DMSO dispersion was slowly added into 25 ml of ANFs/DMSO dispersion. Afterward, the mixture solution was vigorously stirred at room temperature for 1 h and a suspension of GO/ANFs was obtained. Then, 50 ml of deionized (DI) water was added and the reaction was heated to 80 °C and kept stirred for 2 h. GO/ANFs nanocomposite paper were prepared by filtration of the obtained solution through a pol (vinylidene fluoride) (PVDF) (47 mm in diameter, 0.22 μm pore size) film and washing three times with DI water to eliminate impurities, followed with air drying. The GO/ANFs nanocomposite paper was finally peeled off from the filter film. It was placed between two glass plates and dried in air at 80 °C for 72 h. For comparison, GO nanopaper were prepared according to the literature[6, 7].

4.1 Thermal reduced GO/ANFs (TRGO/ANFs) nanocomposite paper

For thermal reduction, the GO/ANFs nanocomposite paper, which is placed between two glass plates, were annealing at 220°C in a vacuum oven for 2 h.

4.2 Chemical reduced GO/ANFs (CRGO/ANFs) nanocomposite paper

For chemical reduction, the GO/ANFs nanocomposite papers were reduced by immersing the nanocomposite papers into HI acid at 80°C for 2h. Subsequently, the papers were washed with sodium bicarbonate solution, DI water and dried at 100°C for 12h.

5 Characterizations and instruments

Fourier transform infrared (FT-IR) spectra were recorded on a Perkine-Elmer Paragon 1000PC spectrometer. X-ray powder diffraction (XRD) patterns were recorded on a D/max-2200/PC (Japan Rigaku Corp.) using CuKα radiation (λ=1.5418 Å). Thermogravimetric analysis (TGA) was performed in nitrogen with a Perkin-Elmer TGA 2050 instrument at a heating rate of 20 °C/min. AFM images were obtained by digital E-Sweep Atomic Force Microscope in tapping mode. The tensile fracture surfaces were characterized by scanning electron microscope (SEM) (JSM-7401F). The morphologies of ANFs and GO were obtained by using transmission electron microscopy (TEM) (JEOL2100F).

5.1 Tensile test for RGO/ANFs nanocomposite paper

The tensile properties of the nanocomposite papers were measured with an Instron 4465 instrument at room temperature with a humidity of about 25% at a crosshead speed of 4 mm/min and an initial gauge length 20 mm, samples were cut into strips of 30 mm × 3mm using a razor blade, and five strips were measured for each sample.

5.2 Electrical conductivity test for RGO/ANFs nanocomposite paper

The electric conductivity of the nanocomposite papers was determined by a four-probe method (SB100A/21A, SH-METER) under a sample platform (SB120/2, SH-METER) equipped with parallel probes (probe spacing: 1mm). The electrical conductivities nanocomposite paper (σ, S/m) were obtained according the sheet resistivity (ρ, $\Omega \cdot$m), $\sigma = 1/\rho$.

The sheet resistivity (ρ, $\Omega \cdot$m) of nanocomposite paper were calculated by the follow formula:

$$\rho = \frac{\pi}{\ln 2} \cdot \frac{V}{I} \cdot d \cdot f(a)$$

, where ρ ($\Omega \cdot$m) is the sheet resistivity of nanocomposite paper, V (V) is the generated voltage, I (A) is the electric current provided by constant current source, d (m) is the thickness of nanocomposite paper and $f(a)$ is correction factor ($f(a) \approx 1$).

6. Characterization of GO

As shown in **Fig.S1a**, the XRD pattern of GO shows an evident peak at $2\theta = 9.41^{\circ}$, corresponding to a *d*-spacing of 0.94 nm, due to the inter-lamellar water trapped between GO nanosheets, [8]. **Fig.S1c** and **1Sd** depict the typical AFM and TEM images of the obtained layered GO nanosheets. The thickness, determined from the height profile of the AFM image, Fig.**1Sd**, is around ~ 0.57 nm, which is consistent with the data reported in the literature, indicating that the formation of the single layered GO[9].

From **Fig.S2**, the fracture edges of GO and TRGO nanopapers both exhibited the layered structure through the entire cross-section. The results demonstrated the GO can be assembled to form highly ordered macroscopic structures under vacuum filtration-induced directional flow. After thermal reduction, the layered structure of nanopaper was kept.

7 Characterizations of ANFs

The bulk macroscale Kevlar 49 fibers can be effectively split into aramid nanofibers by deprotonation in the solution system of DMSO and KOH. The process of splitting the bulk Kevlar 49 macroscale fibers into nanofibers is likely to occur by abstraction of mobile hydrogen from amide groups and substantial reduction the interaction of hydrogen bonds between the polymer chains[5, 10-12]. The electrostatic repulsion between the polymer chains facilitates the formation of ANFs. However, the extent of this destruction is limited and does not appear to proceed down to the level of individual polymer chains due to hydrophobic attraction and π-π stacking in the polymer backbone[5, 12]. The SEM, AFM and TEM images offer the direct information of the production of ANFs **(Fig.S3 and S4)**. The Kevlar 49 macroscale fibers were splitting into the ANFs with the width ranged from 20 to 50 nm.

8 Preparation of ANFs nanopapers

By deprotonating process in solvent system of KOH and DMSO, bulk aramid macroscale fibers were split into the ANFs. As-prepared ANFs exhibited the high reactivity and can be acted as high-performance polymeric building blocks. It’s worth noting that there is a gel phenomenon of when the ANFs/DMSO dispersion was added into the DI water (Fig.S6).

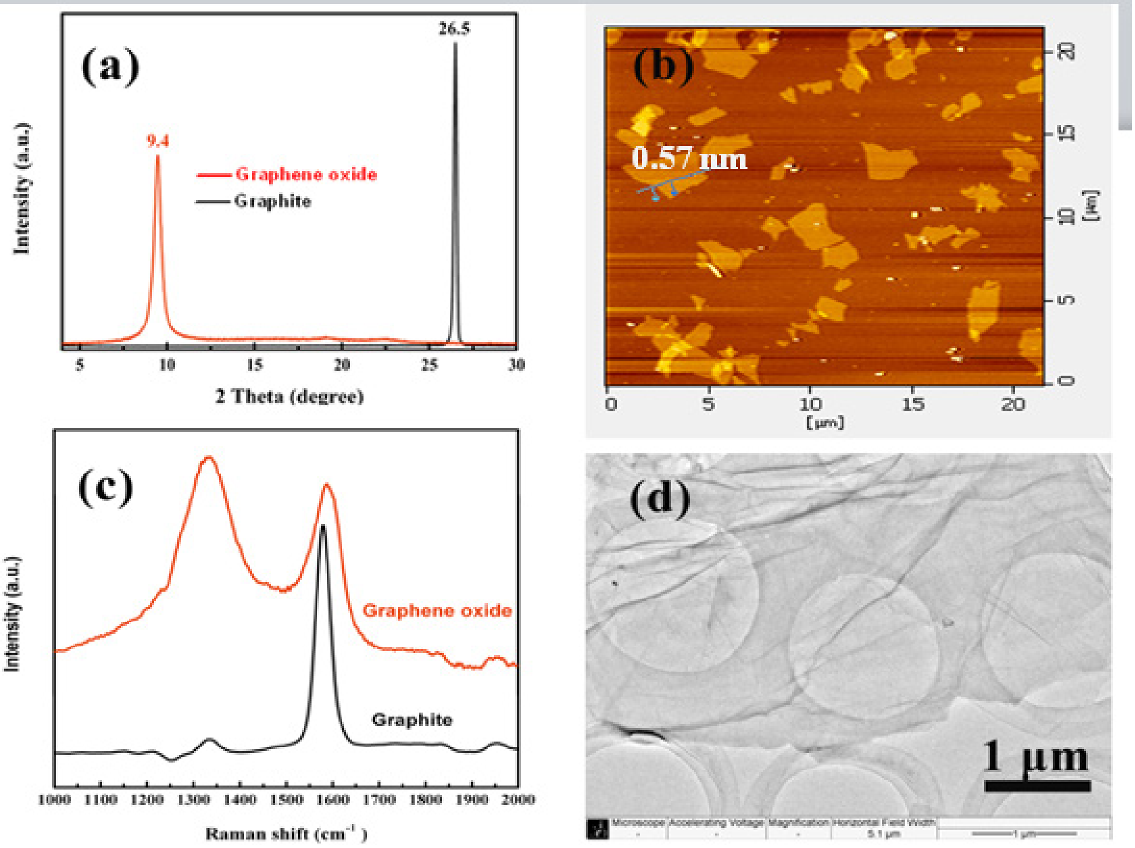

Fig.S1 (a) XRD pattern of GO nanosheets and graphite, (b) typical AFM image of GO nanosheets, (c) Raman spectra of GO nanosheets and pristine graphite, and (d) a typical TEM image of GO nanosheets

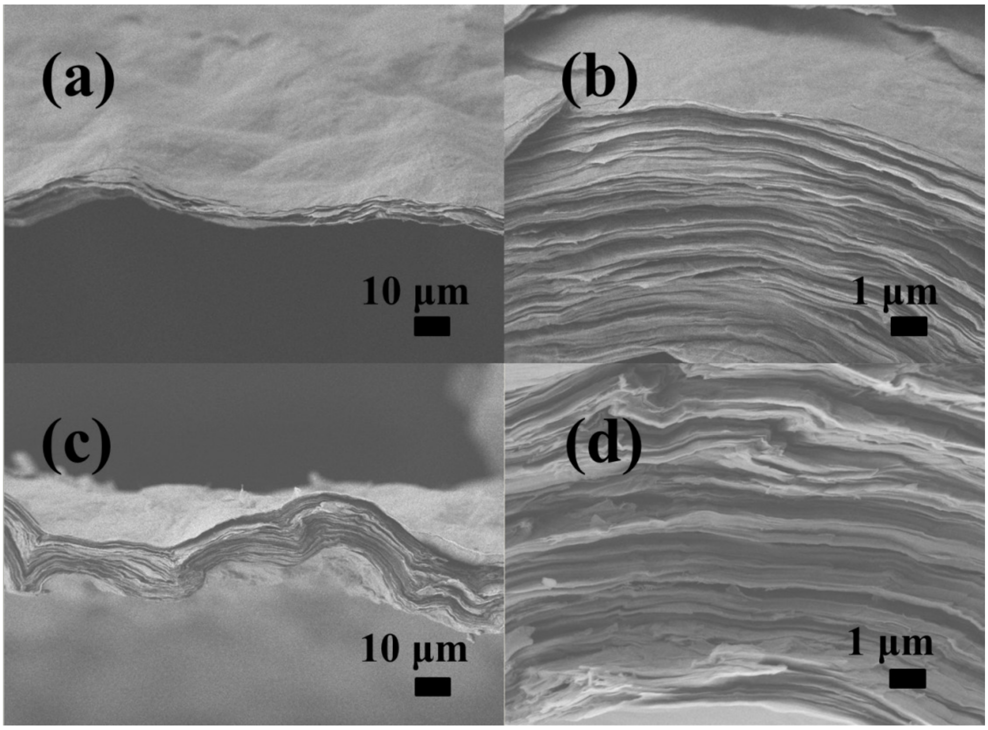

Fig.S2 SEM images of the fracture surfaces of **(a, b)** GO and (**c, d)** TRGO nanopapers with different magnifications

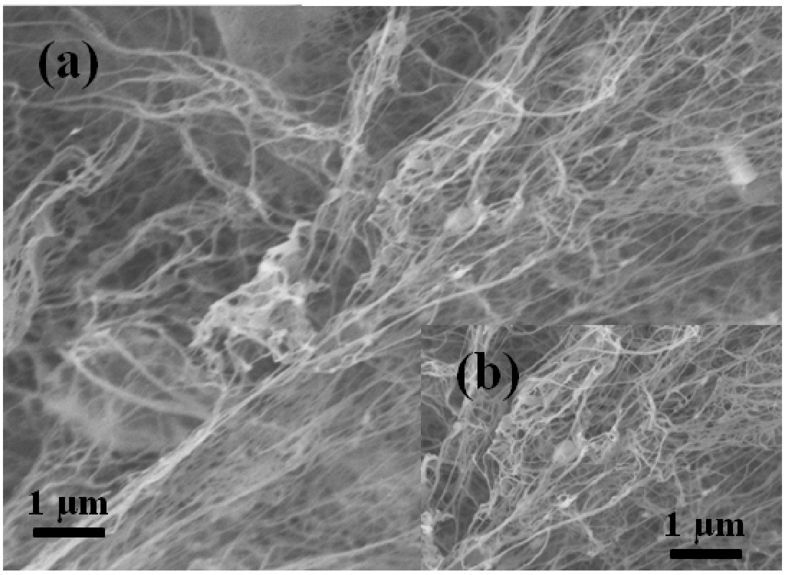

Fig.S3 (a) SEM images of ANFs obtained by freeze-drying (inset: **(b)** partial enlarged view of **(a)**)

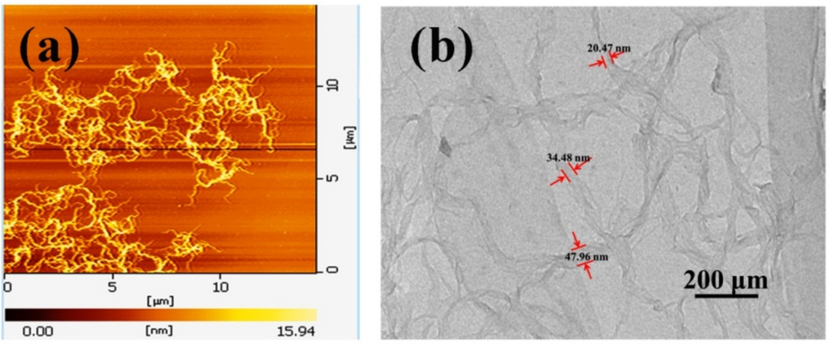

Fig.S4 (a) AFM image of ANFs, and **(b)** typical TEM image of ANFs

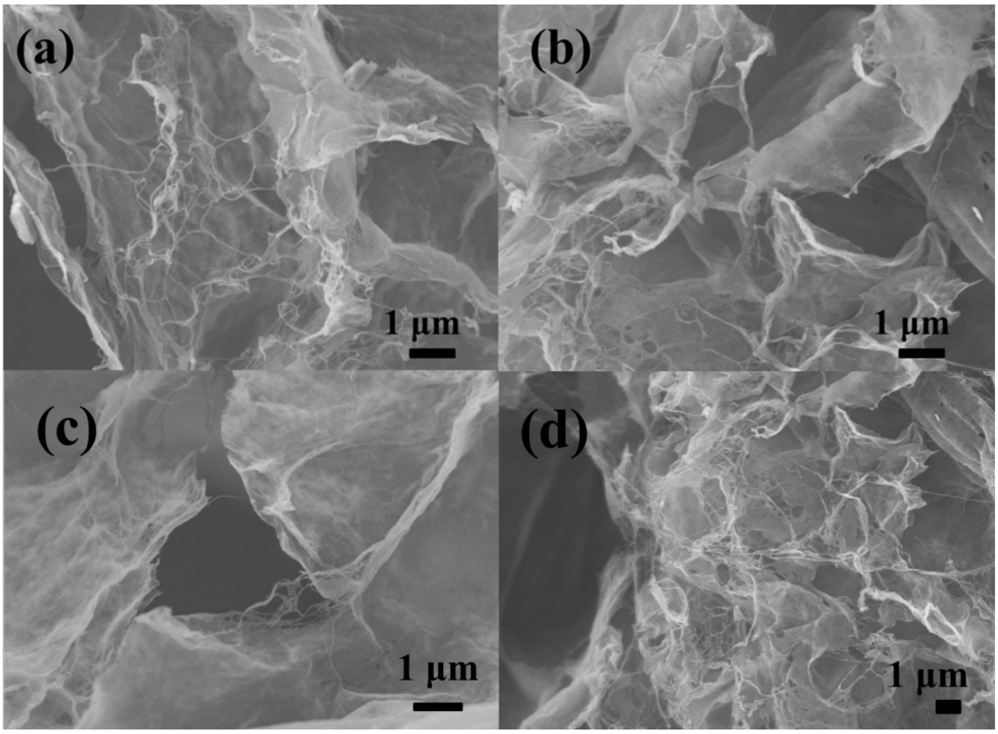

Fig.S5 (a, b, c, and d) SEM images of the GO/ANFs flocculation

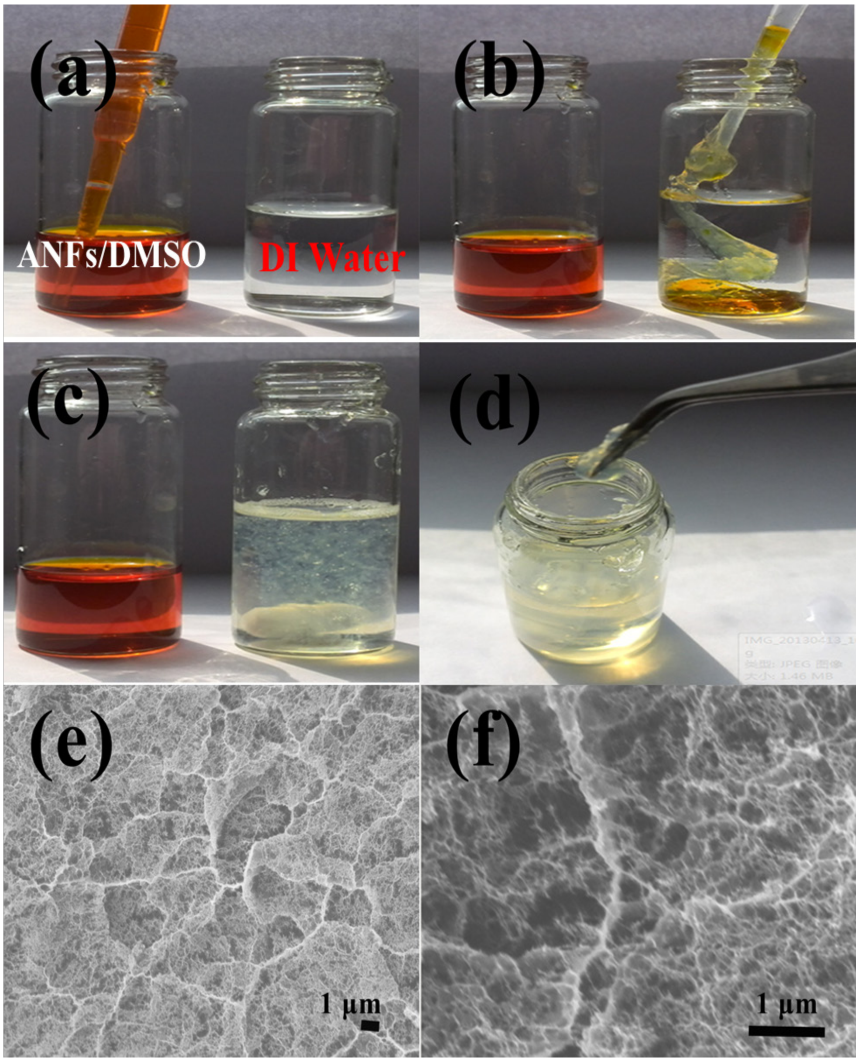

Fig.S6 (a) ANFs/DMSO dispersion and DI water, **(b)** the gel phenomenon of ANFs with the ANFs/DMSO dispersion added into the DI water, **(c)** ANFs/DMSO dispersion (left) and the ANFs suspension liquid dispersion (right), **(d)** the ANFs gel, **(e)** SEM image of ANFs gel with network structures, and **(f)** partial enlarged view of (e)

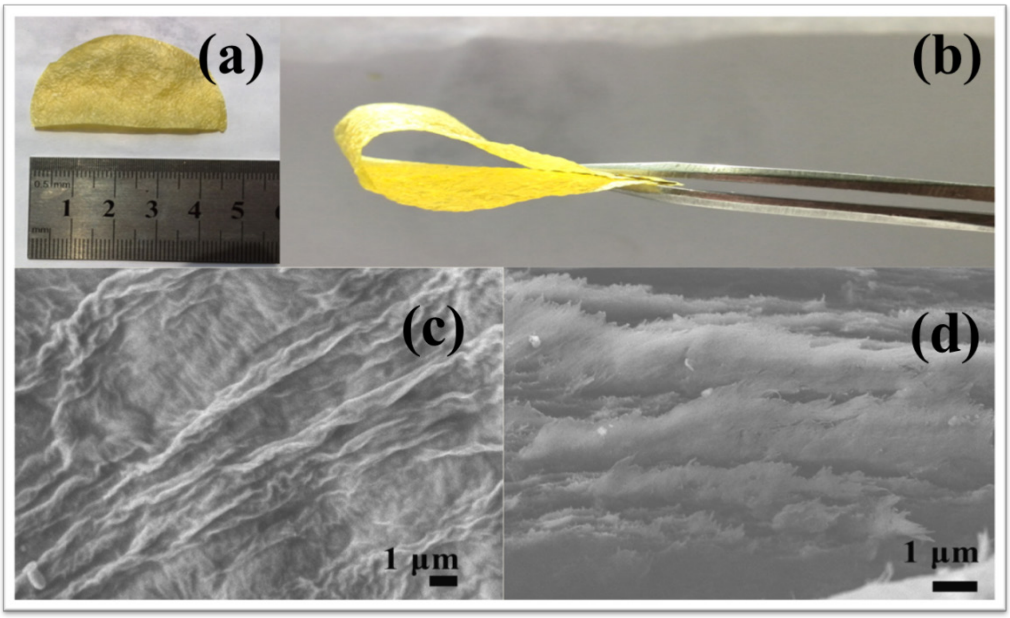

Fig.S7 (a) the dried ANFs nanopaper fabricated by vacuum filtration, (b) the bended ANFs nanopaper, (c) SEM image of the surface of ANFs nanopaper, and (d) SEM image of the fracture surface of the ANFs nanopaper

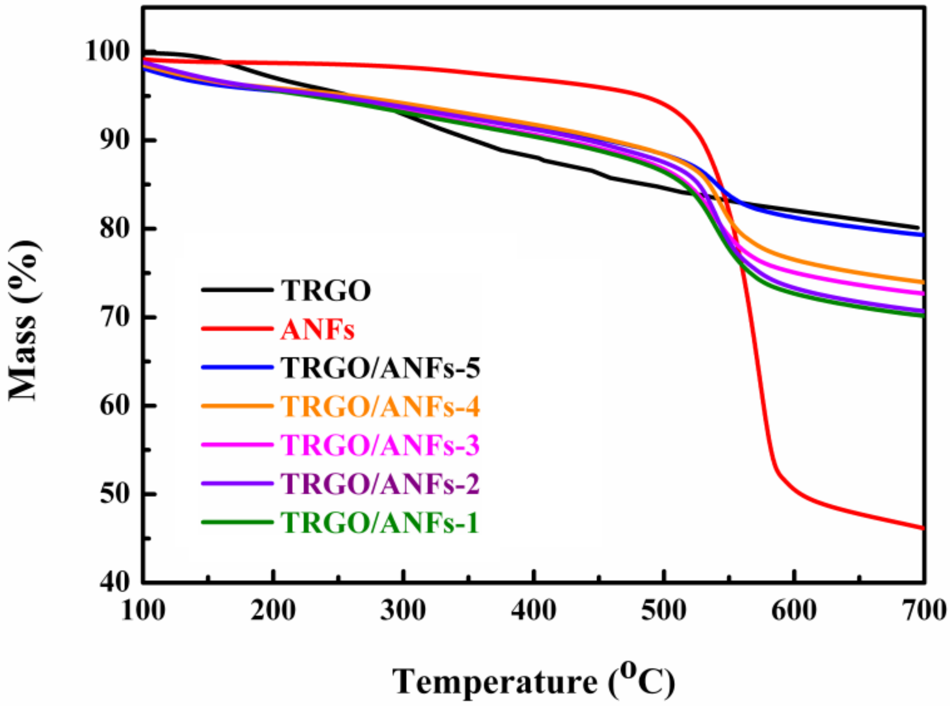

Fig.S8 TGA curves of RGO, ANFs, TRGO/ANFs-1, TRGO/ANFs-2, TRGO/ANFs-3, TRGO/ANFs-4 and TRGO/ANFs-5

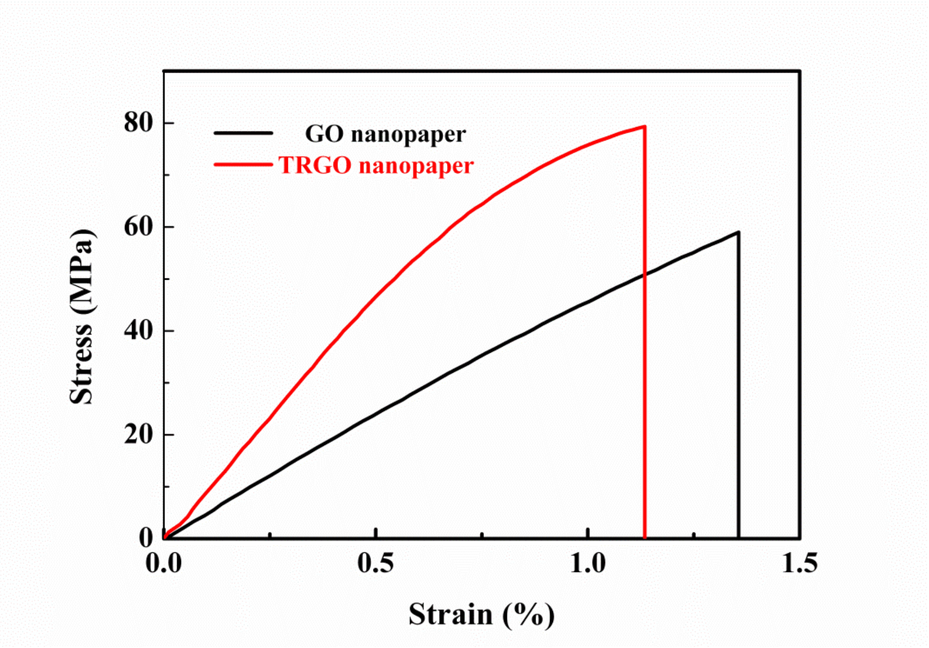

Fig.S9 Typical strain-stress curves for the GO and TRGO nanopapers

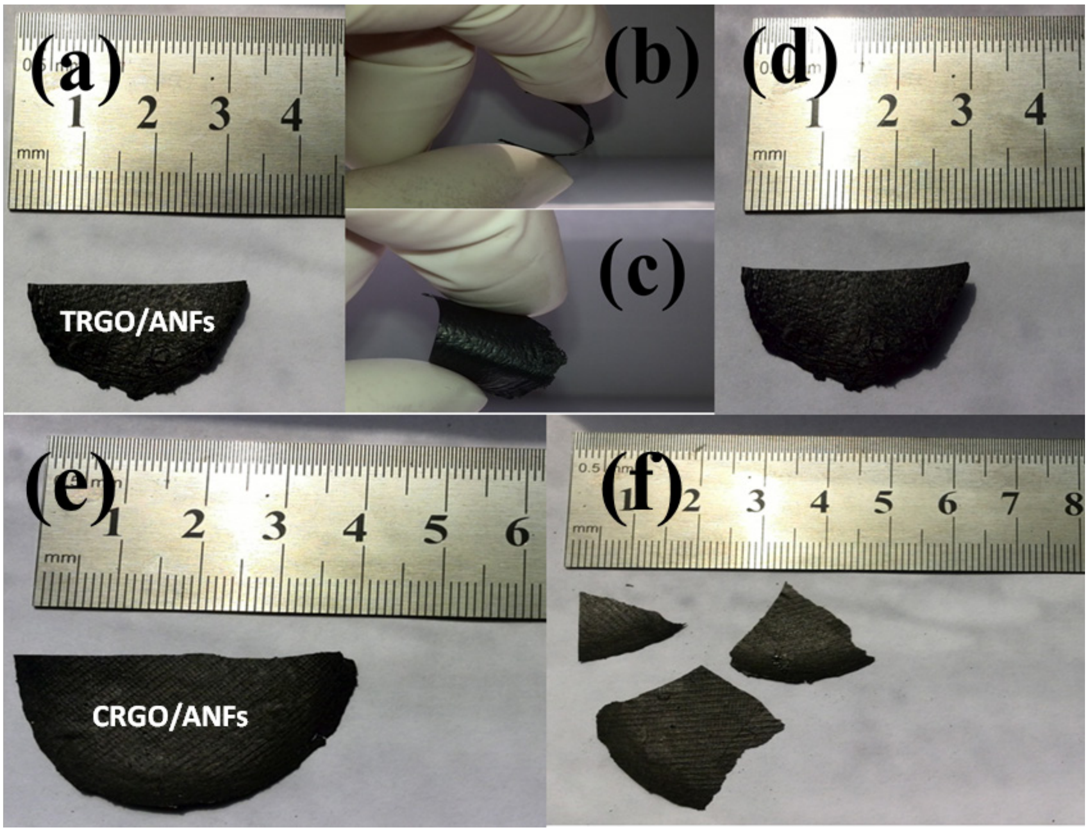

Fig.S10 Photographs of (a) the TRGO/ANFs-5 nanocomposite paper, (b, and c) the bended TRGO/ANFs-5 nanocomposite paper under different bending angles, (d) the TRGO/ANFs-5 nanocomposite paper after bending ,(e) the CRGO/ANFs-5 nanocomposite paper, (f) the broken CRGO/ANFs-5 nanocomposite paper after bending with a small bending angle

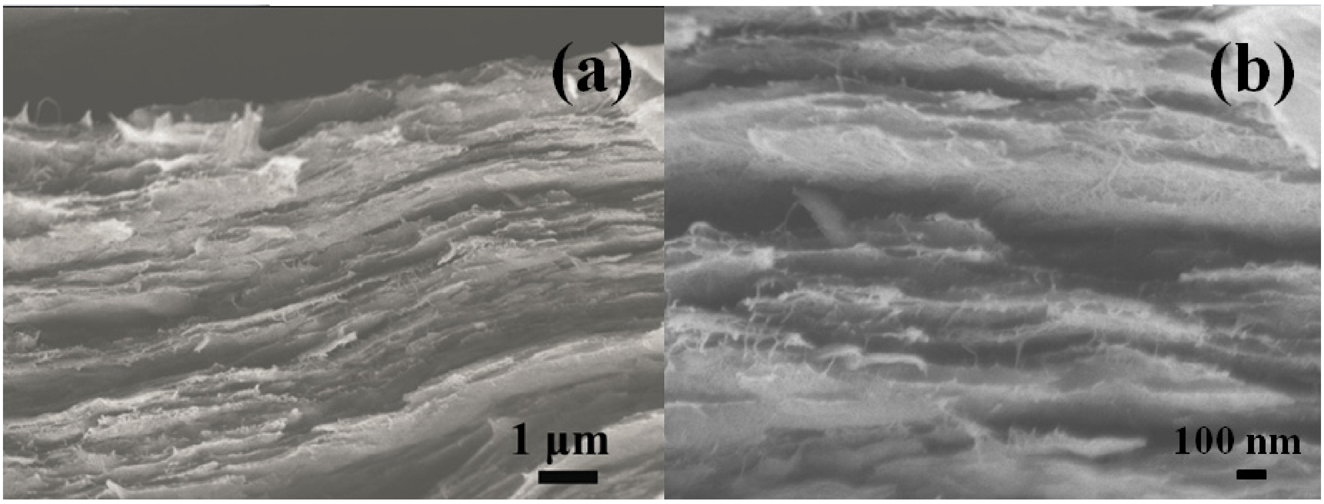

Fig.S11 SEM images of the fracture surface of the TRGO/ANFs-5 nanocomposite paper under different magnifications

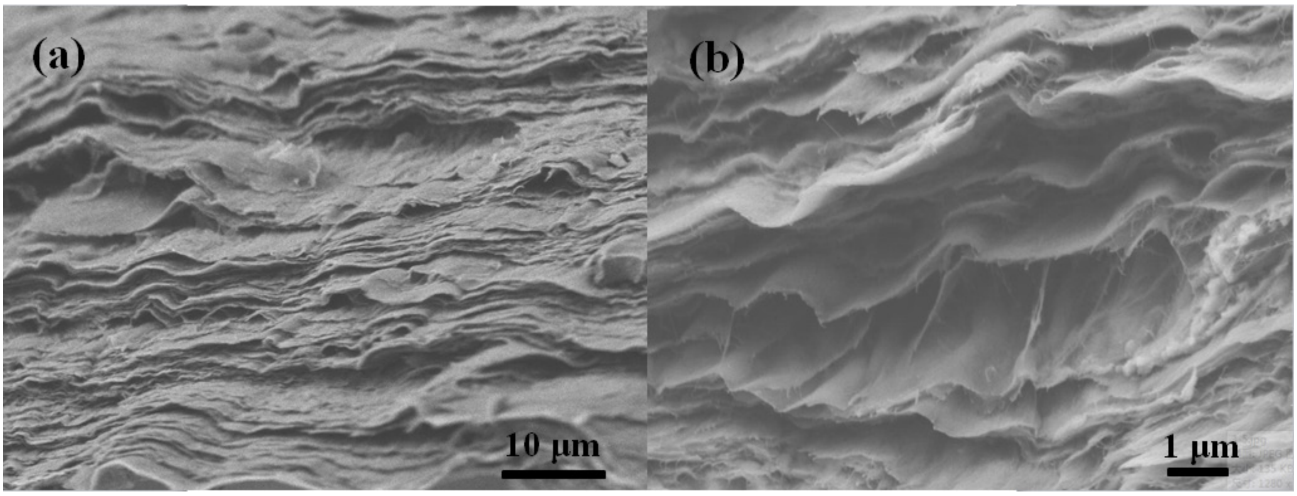

Fig.S12 SEM images of the fracture surface of the CRGO/ANFs-5 nanocomposite paper under different magnifications

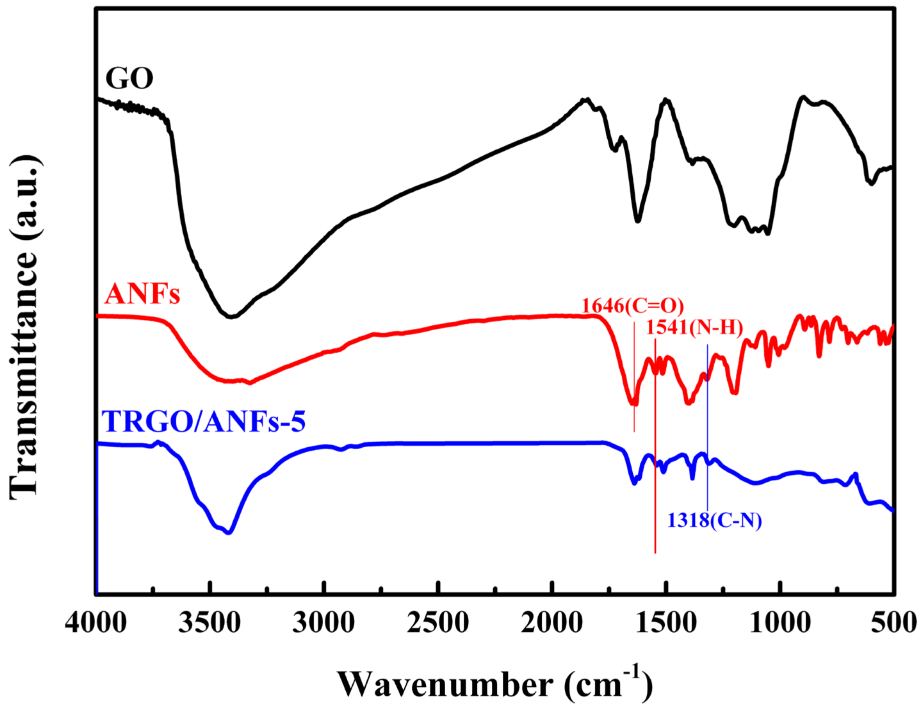

Fig.S13 FT-IR spectra of GO, ANFs and TRGO/ANFs

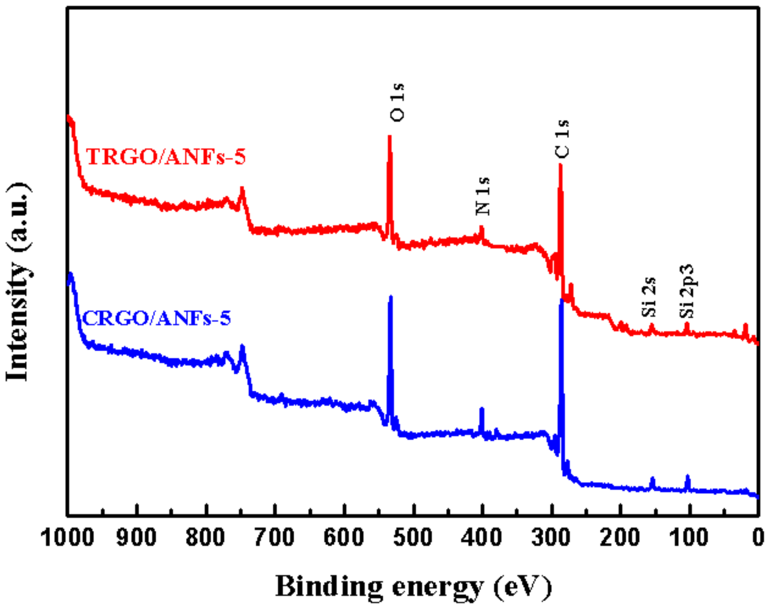

Fig.S14 XPS spectrum of CRGO/ANFs-5 and TRGO/ANFs-5 nanocomposite paper

References

1. N. I. Kovtyukhova, P. J. Ollivier, B. R. Martin, T. E. Mallouk, S. A. Chizhik, E. V. Buzaneva and A. D. Gorchinskiy, *Chem. Mater.*, 1999, **11**, 771-778.

2. Y. Xu, H. Bai, G. Lu, C. Li and G. Shi, *J. Am. Chem. Soc.*, 2008, **130**, 5856-5857.

3. S. M. Liff, N. Kumar and G. H. McKinley, *Nat. Mater.*, 2007, **6**, 76-83.

4. Y. Wang, Z. Shi, J. Fang, H. Xu and J. Yin, *Carbon*, 2011, **49**, 1199-1207.

5. M. Yang, K. Cao, L. Sui, Y. Qi, J. Zhu, A. Waas, E. M. Arruda, J. Kieffer, M. D. Thouless and N. A. Kotov, *ACS Nano*, 2011, **5**, 6945-6954.

6. D. A. Dikin, S. Stankovich, E. J. Zimney, R. D. Piner, G. H. B. Dommett, G. Evmenenko, S. T. Nguyen and R. S. Ruoff, *Nature*, 2007, **448**, 457-460.

7. H. Chen, M. B. Müller, K. J. Gilmore, G. G. Wallace and D. Li, *Adv. Mater.*, 2008, **20**, 3557-3561.

8. S. Stankovich, D. A. Dikin, R. D. Piner, K. A. Kohlhaas, A. Kleinhammes, Y. Jia, Y. Wu, S. T. Nguyen and R. S. Ruoff, *Carbon*, 2007, **45**, 1558-1565.

9. S. Park and R. S. Ruoff, *Nat Nano*, 2009, **4**, 217-224.

10. M. Takayanagi, T. Kajiyama and T. Katayose, *J Appl Polym Sci*, 1982, **27**, 3903-3917.

11. R. R. Burch, W. Sweeny, H. W. Schmidt and Y. H. Kim, *Macromolecules*, 1990, **23**, 1065-1072.

12. R. R. Burch and L. E. Manring, *Macromolecules*, 1991, **24**, 1731-1735.